The role of a localized modulation of $\chi^{(2)}$ in Čerenkov second harmonic generation in nonlinear bulk medium

Yan Sheng[1,*], Vito Roppo[1], Ksawery Kalinowski[1], and Wieslaw Krolikowski[1]

[1] *Laser Physics Center, Research School of Physics and Engineering, Australian National University, ACT 0200, Australia*

[*] *Corresponding author: ysh111@physics.anu.edu.au*

Compiled July 24, 2012

We study the second harmonic generation in quadratic nonlinear media with localized spatial modulation of $\chi^{(2)}$ response. We demonstrate that the emission of Čerenkov second harmonic takes place only when the fundamental beam illuminates the region of $\chi^{(2)}$ variation. This proves that the sharp modulation of the $\chi^{(2)}$ nonlinearity constitutes a sufficient condition for the emission of Čerenkov second harmonic in bulk materials. Our calculations are in excellent agreement with simple analytical approach utilizing the concept of reciprocal vectors representing the Fourier spectrum of the modulation of $\chi^{(2)}$.

OCIS codes: 190.2620, 190.4410, 220.4000

Nonlinear optical Čerenkov emission represents the type of noncollinear parametric process where the direction of the generated wave is defined by the longitudinal phase matching condition [1]. In the simplest case of Čerenkov second harmonic generation (ČSHG), the radiation of the doubled frequency is observed at the angle defined as $\theta = \cos^{-1}(2k_1 \cos\alpha/k_2)$, where k_1 and k_2 denote the wave vectors of the fundamental and the second harmonic (SH) waves, respectively, and α is the incident angle of the fundamental wave [see Fig. 1(a)]. Recently the ČSHG has attracted lots of attention because of the efficient noncollinear SHG eliminating the necessity of filtering out the incident wave, an valuable feature in all-optical signal processing. Moreover, the ČSHG enables the spatial control of the generated wave front, e.g. forming the radially polarized Bessel beam [2,3]. So far the ČSHG has been realized in bulk ferroelectric crystals with 180^o antiparallel domains [4–7], or in waveguide geometries utilizing the automatic fulfillment of phase-matching condition involving guided fundamental and radiation harmonic modes [8,9].

Regarding ČSHG in bulk ferroelectric crystals, it has been found by using tightly focused fundamental beams that effective ČSHG takes place only in the vicinity of the ferroelectric domain wall separating antiparallel ferroelectric domains [10–12]. This property has already been shown to be extremely useful as an efficient tool for a non-destructive diagnostics of three-dimensional domain patterns in ferroelectric crystals [11–13].

For a long time the physical origin of this enhancement of ČSHG by a ferroelectric domain structure has been a subject of controversy. On one hand, it was suggested that the periodic change of sign of second-order nonlinearity $\chi^{(2)}$ serves as a source of reciprocal lattice vectors which can enable efficient ČSHG via non collinear quasi-phase matching [7,14]. On the other hand, it was claimed that the distortion of crystal lattice across the domain wall may induce local enhancement of $\chi^{(2)}$, which consequently leads to stronger ČSHG on the wall [10,15].

In this letter, we aim to resolve this issue by studying the Čerenkov second harmonic generation in an optical bulk medium consisting of two semi-infinite regions with different strengths and/or signs of the nonlinearity $\chi^{(2)}$. While the actual ferroelectric domain wall may indeed lead to some modification of the nonlinearity tensor [10], we concentrate here on much simpler situation of a sharp variation of the value of $\chi^{(2)}$. Consequently we reveal that abrupt change of $\chi^{(2)}$ in transverse direction constitutes a *sufficient* condition for the emission of ČSHG. In fact, an individual spatially localized change of $\chi^{(2)}$ can provide a *continuous* set of reciprocal vectors leading to efficient ČSHG. Therefore, a periodic modulation of $\chi^{(2)}$ is no longer necessary. We also discuss the strong sensitivity of the Čerenkov signal to the width and incidence angle of the fundamental beam. we may remove this last sentence to save some space

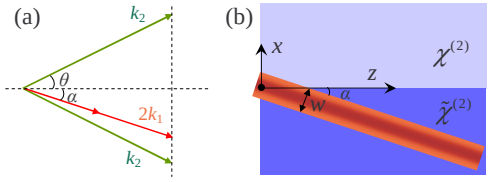

Fig. 1. (Color online) (a) Phase matching diagram of Čerenkov second harmonic generation. (b) Schematic of the simulation with SHG in optical media containing two layers of different nonlinear responses: $\chi^{(2)}$ and $\tilde{\chi}^{(2)}$.

As shown in Fig. 1(b), we consider two semi-infinite regions with different quadratic nonlinear responses $\chi^{(2)}$ and $\tilde{\chi}^{(2)}$. The fundamental beam (λ=1.2 μm, beam width w) propagates in the medium at an angle α against the boundary. To avoid any possible influence of the discontinuity in the linear polarization [16], the refractive index of the system is assumed to be homogenous.

The system of corresponding wave equations for the

fundamental and second harmonics reads [17]:

$$\frac{\partial E_1}{\partial z} = \frac{i}{2k_1}\nabla_\perp^2 E_1 - i\frac{\omega_1^2\chi^{(2)}(x)}{k_1 c^2}E_1^* E_2 e^{i(k_2-2k_1)z},$$
$$\frac{\partial E_2}{\partial z} = \frac{i}{2k_2}\nabla_\perp^2 E_2 - i\frac{\omega_2^2\chi^{(2)}(x)}{2k_2 c^2}E_1^2 e^{i(2k_1-k_2)z}, \quad (1)$$

where ω_1 and ω_2=2ω_1 are the fundamental and SH frequencies, respectively. We assumed that the field can be decomposed as a superposition of these two frequencies, with stationary envelopes and fast oscillating term:

$$E = \quad E_1(x,z)e^{i(k_1 z-\omega_1 t)} + E_2(x,z)e^{i(k_2 z-\omega_2 t)} + c.c. \quad (2)$$

In this model only the contributions from the diffraction and the quadratic nonlinearity are included, and no transient behavior or interface enhanced linear and/or nonlinear effects are considered.

The second harmonic generation is analyzed by numerically solving the Eq. (1) via standard FFT-based beam propagation method. We use the dispersion data of $LiNbO_3$ crystal [18]. In Fig. 2 we depict both near- and far-field SH distributions versus the propagation distance, calculated with the fundamental beam propagating at $\alpha = 0°$ along three types of $\chi^{(2)}$ boundary in nonlinear media. The first row shows the SHG when the nonlinearity $\chi^{(2)}$ switches its sign across the boundary, i.e. $\chi^{(2)} = -\tilde{\chi}^{(2)} = \chi_0^{(2)}$. The strong emission of ČSHG is observed around $\pm 28.6°$ in the far field, agreeing well with the calculated Čerenkov angle for $LiNbO_3$ crystal [18]. The SH energy grows with the interaction length, a character of the phase matched nature of this nonlinear Čerenkov emission. The simulation actually represents the experimental observation of ČSHG on the single domain wall of ferroelectric crystal, across which the $\chi^{(2)}$ switch its sign. In the second row of Fig. 2, we display the SHG calculated with $\chi^{(2)}$ changing its value from $\chi_0^{(2)}$ to zero. This corresponds to a situation when the nonlinear response is nonzero in only one part of the medium. It is interesting that the Čerenkov harmonic is generated in exactly the same manner as at the domain wall $\pm\chi_0^{(2)}$, except for lower intensity of the generated signal. For comparison, the bottom row illustrates the SHG in a homogenous nonlinear medium, i.e. $\chi^{(2)} = \tilde{\chi}^{(2)} = \chi_0^{(2)}$. In this case only the forward (phase mismatched) SH signal is present while the noncollinear ČSHG completely disappears. This behavior indicates that the existence of any spatial modulation of the second-order nonlinearity $\chi^{(2)}$ constitutes the sufficient condition for efficient generation of Čerenkov signal.

This is further confirmed by the calculations depicted in Fig. 3 where we show the effect of the spatial profile of the of $\chi^{(2)}$ variation on the emitted ČSHG. In the simulations we modeled the quadratic nonlinearity as

$$\chi^{(2)}(x) = \frac{2\chi_0^{(2)}}{\pi}\tan^{-1}(Dx), \quad (3)$$

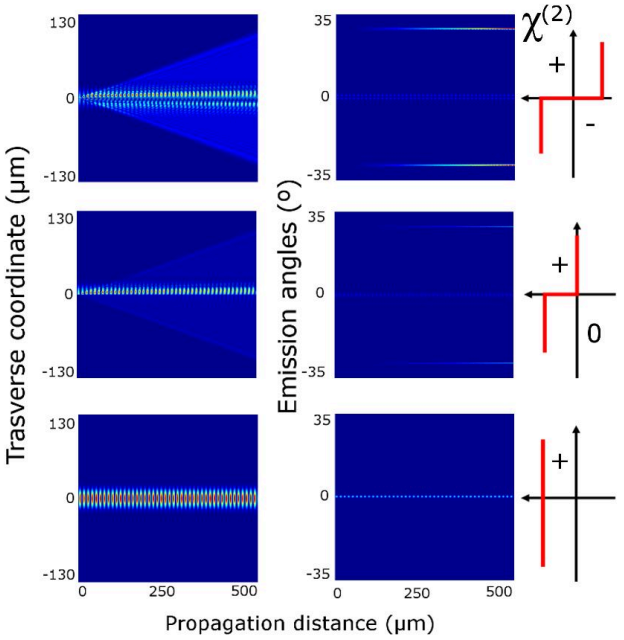

Fig. 2. (Color online) Near-field (left column) and far-field (right column) intensity distribution of the SHG in composite media with fundamental beam propagating along boundary separating different strengths of the nonlinearity. The nonlinearity modulation across the boundary is given as (from top to bottom): $\chi^{(2)}/-\chi^{(2)}$, $\chi^{(2)}/0$ and $\chi^{(2)}/\chi^{(2)}$ (homogeneous medium).

where D represents the steepness of $\chi^{(2)}$ variation. For $D \gg 1$ the function Eq.(3) approaches the step function. In actual physical setting such spatial modulation of $\chi^{(2)}$ could represent simple model of ferroelectric domain wall separating nonlinear responses of opposite signs. In simulations we used $D = 10^6, 10^7, 10^8$ and 10^9 [Fig. 3(a)]. It is seen from Fig. 3(b) that the profile of $\chi^{(2)}$ variation does not affect the Čerenkov angle. This agrees with the fact that the direction of Čerenkov emission depends solely on the dispersion properties of the medium. However, the intensity of Čerenkov signal is very sensitive to the profile of $\chi^{(2)}$ modulation. The sharper the change of $\chi^{(2)}$, the stronger the Čerenkov signal. This effect could be of interest to the study of the properties of ferroelectric domains especially when combined with Čerenkov-based domain visualization [11, 12].

It is easy to interpret the results obtained above if we consider the nonlinear Čerenkov radiation as a fully phase matched process, i.e. the missing momentum in the transverse direction is compensated for by the reciprocal vectors associated with the $\chi^{(2)}$ variation. In this case the intensity of ČSHG should be proportional to the square of the Fourier coefficient $M(\kappa)$ of the nonlinearity spectrum corresponding to the transverse wave vector κ such that $\kappa/k_2 = \sin\theta$. In our case

$$M(\kappa) = \chi_0^{(2)}\frac{i}{\kappa}\exp^{-|\kappa/D|}. \quad (4)$$

With regard to Fig. 3 it is now obvious that $|M(\kappa)|$ increases with D, approaching the maximum $M(\kappa)_{max} = i\chi_0^{(2)}/\kappa$ for the step jump of $\chi^{(2)}$. The Eq. (4) also explains the difference in the strengths of the signals generated by $\chi^{(2)}/-\chi^{(2)}$ and $\chi^{(2)}/0$ boundaries (the top two rows of Fig. 2). The weaker Čerenkov signal in the latter case comes about because the corresponding Fourier coefficient is two times smaller than that of the former's.

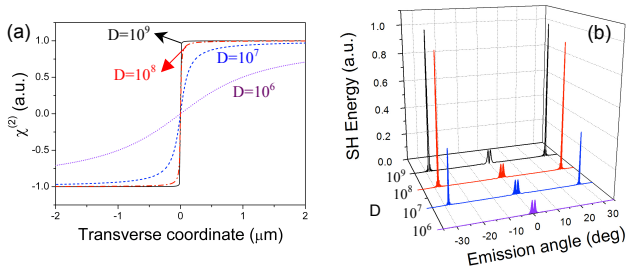

Fig. 3. (Color online) (a) Illustrating different spatial profiles of the $\chi^{(2)}$ modulation across the boundary. (b) The angular profile of the SH emission. Two peaks located at $\theta = \pm 28.6°$ represent Čerenkov signals. Notice the strength of the emission increasing with D.

Let's now consider the SHG in a more general geometry of interaction, i.e. the fundamental beam propagates along an arbitrary direction ($\alpha \neq 0°$). Figure 4(a) shows the result where the straight line in the graph represents the collinear phase mismatched emission, while the two curves represent the Čerenkov radiations. It is worth noting that the Čerenkov emission at a single $\chi^{(2)}$ boundary follows the scenario observed in experiments with multiple domain walls in periodically poled ferroelectric crystals [7]. Firstly, the emission angle θ increases with the incident angle, according to the relation $k_2 \cos\theta = 2k_1 \cos\alpha$. Secondly, while the Čerenkov signals are always generated symmetrically with respect to the boundary of the $\chi^{(2)}$, they show asymmetric intensity distribution. The signal emitted in the direction closer to that of the fundamental beam is always stronger. This is a consequence of the fact that this signal involves a smaller phase mismatch (smaller κ) in the transverse direction, which corresponds to a larger Fourier coefficient. The monotonic decrease of the signal with increasing α is due to the shortening of the effective interaction length determined by the overlap of the fundamental beam and the $\chi^{(2)}$ boundary.

In Fig. 4(b) we display the effect of the beam size of the fundamental wave on the ČSHG. We keep the peak intensity of the wave constant while varying the beam width. It is seen that at first the Čerenkov signal grows with the increase of beam size owing to the higher pump power. However, it quickly reaches saturation since that only the part of the fundamental beam in the immediate vicinity of the $\chi^{(2)}$ boundary contributes to the emission.

We have to point out that our experimental attempt to observe visually the Čerenkov harmonic from single-domain $LiNbO_3$ samples using intensities up to the damage threshold failed. We think that several publications reporting Čerenkov SHG in homogenous crystal [19, 20] may be associated with the structure defects of the crystal, which can also introduce a localized $\chi^{(2)}$ modulation.

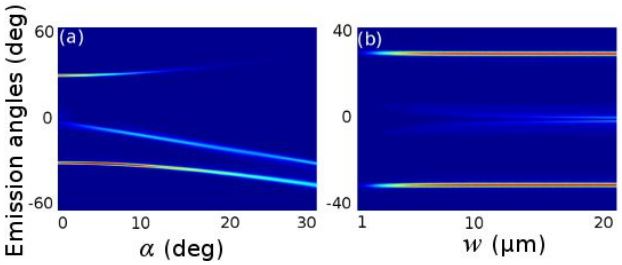

Fig. 4. (Color online) (a) The SHG as a function of incident angle α of the fundamental wave. The Čerenkov emission is represented by the two outmost curves. The central line depicts the forward SH signal. (b) The effect of the beam width w on the Čerenkov SHG. The calculations correspond to $D = 10^9$ in Eq. (3).

In conclusion, we have studied the role of a localized spatial modulation of $\chi^{(2)}$ in the Čerenkov second harmonic generation. We show that the very variation of $\chi^{(2)}$ constitutes a sufficient condition for the nonlinear Čerenkov emission. This effect is caused by the presence of a continuous set of reciprocal wave vectors associated with the $\chi^{(2)}$ modulation which enables satisfying the full phase matching condition of the second harmonic generation. The results can be easily generalized to Čerenkov emissions from periodic $\chi^{(2)}$ structure, in which the spectrum of reciprocal vectors is defined by both localized and periodic $\chi^{(2)}$ modulations.

The authors acknowledge the financial supports from Australian Research Council. V. Roppo thanks the Endeavor Award for partial financial support.

References

1. E. Mathieu, ZAMP **20**, 433-439 (1969).
2. S. M. Saltiel, D. N. Neshev, W. Krolikowski, R. Fisher, A. Arie, and Y. S. Kivshar, Phys. Rev. Lett. **100**, 103902 (2008).
3. S. Saltiel, W. Krolikowski, D. N. Neshev, and Y. S. Kivshar, Opt. Express, **15**, 4132-4138 (2007).
4. A. R. Tunyagi, M. Ulex, and K. Betzler, Phys. Rev. Lett. **90**, 243901 (2003).
5. Y. Sheng, S. M. Saltiel, W. Krolikowski, A. Arie, K. Koynov, and Y. Kivshar, Opt. Lett. **35**, 1317-1319 (2010).
6. P. Molina, M. O. Ramirez, B. J. Garcia, and L. E. Bausa, Appl. Phys. Lett. **96,** 261111 (2010).
7. K. Kalinowski, P. Roedig, Y. Sheng, M. Ayoub, J. Imbrock, C. Denz, and W. Krolikowski, Opt. Lett. **37**, 1832-1834 (2012).
8. P. K. Tien, R. Ulrich, and R. J. Martin, Appl. Phys. Lett. **17**, 447-450 (1970).

9. Y. Zhang, Z. D. Gao, Z. Qi, S. N. Zhu, and N. B. Ming, Phys. Rev. Lett. **100**, 163904 (2008).
10. A. Fragemann, V. Pasiskevicius, and F. Laurell, App. Phys. Lett. **85**, 375-377 (2004).
11. Y. Sheng, A. Best, H. Butt, W. Krolikowski, A. Arie, and K. Koynov, Opt. Express **16**, 16539 (2010).
12. X. Deng and X. Chen, Opt. Express **18,** 15597 (2010).
13. K. Kalinowski, Q. Kong, V. Roppo, A. Arie, Y. Sheng, and W. Krolikowski, Appl. Phys. Lett. **99**, 181128 (2011).
14. S. M. Saltiel, Y. Sheng, N. Voloch-Bloch, D. N. Neshev, W. Krolikowski, A. Arie, K. Koyonov, Y. S. Kivshar, IEEE J. Quantum Electron. **45**, 1465-1472 (2009).
15. X. Deng, H. Ren, Y. Zheng and X. Chen, arXiv:1005.2925 (2010).
16. N. Bloembergen, J. Opt. Soc. Am. **70**, 1429-1436 (1980).
17. R. W. Boyd, *Nonlinear Optics* (Academic Press, 2007).
18. G. J. Edwards and M. Lawrence, Opt. Quantum Electron. **16**, 373-375 (1984).
19. A. A. Kaminskii, H. Nishioka, K. Ueda, W. Odajima, M. Tateno, K. Sasaki, and A. V. Butashin, Quantum Electron. **26**, 381-382 (1996).
20. V. Vacaitis, Opt. Commun. **209**, 485-490 (2002).

Informational Fourth Page

References

1. E. Mathieu, "Conditions for quasi Cerenkov radiation, generated by optical second harmonic polarisation in a nonlinear cristal", ZAMP **20**, 433-439 (1969).
2. S. M. Saltiel, D. N. Neshev, W. Krolikowski, R. Fisher, A. Arie, and Y. S. Kivshar, "Generation of second-harmonic conical waves via nonlinear Bragg diffraction", Phys. Rev. Lett. **100**, 103902 (2008).
3. S. Saltiel, W. Krolikowski, D. N. Neshev, and Y. S. Kivshar, "Generation of Bessel beams by parametric frequency doubling in annular nonlinear periodic structures", Opt. Express, **15**, 4132-4138 (2007).
4. A. R. Tunyagi, M. Ulex, and K. Betzler, "Noncollinear optical frequency doubling in strontium barium niobate", Phys. Rev. Lett. **90**, 243901 (2003).
5. Y. Sheng, S. M. Saltiel, W. Krolikowski, A. Arie, K. Koynov, and Y. Kivshar, "Čerenkov-type second-harmonic generation with fundamental beams of different polarizations", Opt. Lett. **35**, 1317-1319 (2010).
6. P. Molina, M. O. Ramirez, B. J. Garcia, and L. E. Bausa, "Directional dependence of the second harmonic response in two-dimensional nonlinear photonic crystals", Appl. Phys. Lett. **96,** 261111 (2010).
7. K. Kalinowski, P. Roedig, Y. Sheng, M. Ayoub, J. Imbrock, C. Denz, and W. Krolikowski, "Enhanced Čerenkov second-harmonic emission in nonlinear photonic structures", Opt. Lett. **37**, 1832-1834 (2012).
8. P. K. Tien, R. Ulrich, and R. J. Martin, "Optical second harmonic generation in form of coherent cerenkov radiation from a thin-film waveguide", Appl. Phys. Lett. **17**, 447-450 (1970).
9. Y. Zhang, Z. D. Gao, Z. Qi, S. N. Zhu, and N. B. Ming, "Nonlinear Čerenkov radiation in nonlinear photonic crystal waveguides", Phys. Rev. Lett. **100**, 163904 (2008).
10. A. Fragemann, V. Pasiskevicius, and F. Laurell, "Second-order nonlinearities in the domain walls of periodically poled $KTiOPO_4$", App. Phys. Lett. **85**, 375-377 (2004).
11. Y. Sheng, A. Best, H. Butt, W. Krolikowski, A. Arie, and K. Koynov, "Three-dimensional ferroelectric domain visualization by Čerenkov-type second harmonic generation", Opt. Express **16**, 16539 (2010).
12. X. Deng and X. Chen, "Domain wall characterization in ferroelectrics by using localized nonlinearities", Opt. Express **18,** 15597 (2010).
13. K. Kalinowski, Q. Kong, V. Roppo, A. Arie, Y. Sheng, and W. Krolikowski, "Wavelength and position tuning of Čerenkov second-harmonic generation in optical superlattice", Appl. Phys. Lett. **99**, 181128 (2011).
14. S. M. Saltiel, Y. Sheng, N. Voloch-Bloch, D. N. Neshev, W. Krolikowski, A. Arie, K. Koyonov, Y. S. Kivshar, "Cerenkov-type second-harmonic generation in two-dimensional nonlinear photonic structures", IEEE J. Quantum Electron. **45**, 1465-1472 (2009).
15. X. Deng, H. Ren, Y. Zheng and X. Chen, "Signifiantly enhanced second order nonlinearity in domain walls of ferroelectric", arXiv:1005.2925 (2010).
16. N. Bloembergen, "Conservation laws in nonlinear optics", J. Opt. Soc. Am. **70**, 1429-1436 (1980).
17. R. W. Boyd, *Nonlinear Optics* (Academic Press, 2007).
18. G. J. Edwards and M. Lawrence, "A temperature dependent dispersion equation for congruently grown lithium niobate", Opt. Quantum Electron. **16**, 373-375 (1984).
19. A. A. Kaminskii, H. Nishioka, K. Ueda, W. Odajima, M. Tateno, K. Sasaki, and A. V. Butashin, "Second-harmonic generation with Cerenkov-type phase matching in a bulk nonlinear $LaBGeO_5$ crystal," Quantum Electron. **26**, 381-382 (1996).
20. V. Vacaitis, "Cerenkov-type phase matching in bulk KDP crystal", Opt. Commun.**209**, 485-490 (2002).